

Article

# Chitosan–Collagen Coated Magnetic Nanoparticles for Lipase Immobilization—New Type of “Enzyme Friendly” Polymer Shell Crosslinking with Squaric Acid

Marta Ziegler-Borowska <sup>1,\*</sup>, Dorota Chelminiak-Dudkiewicz <sup>1</sup>, Tomasz Siódmiak <sup>2</sup>, Adam Sikora <sup>2</sup>, Katarzyna Wegrzynowska-Drzymalska <sup>1</sup>, Joanna Skopinska-Wisniewska <sup>1</sup>, Halina Kaczmarek <sup>1</sup> and Michał P. Marszał <sup>2</sup>

<sup>1</sup> Faculty of Chemistry, Nicolaus Copernicus University in Torun, Gagarina 7, 87-100 Torun, Poland; dorotachelminiak@wp.pl (D.-C.D.); lasia91@wp.pl (K.W.-D.); joanna@chem.umk.pl (J.S.-W.); halina@chem.umk.pl (H.K.)

<sup>2</sup> Faculty of Pharmacy, Collegium Medicum in Bydgoszcz, Nicolaus Copernicus University in Torun, dr A. Jurasza 2, 85-089 Bydgoszcz, Poland; sioodmy@wp.pl (T.S.); sikora.a.e@gmail.com (A.S.); mmars@cm.umk.pl (M.P.M.)

\* Correspondence: martaz@chem.umk.pl; Tel.: +48-56-611-4916

Academic Editor: David D. Boehr

Received: 27 October 2016; Accepted: 10 January 2017; Published: 14 January 2017

**Abstract:** This article presents a novel route for crosslinking a polysaccharide and polysaccharide/protein shell coated on magnetic nanoparticles (MNPs) surface via condensation reaction with squaric acid (SqA). The syntheses of four new types of collagen-, chitosan-, and chitosan–collagen coated magnetic nanoparticles as supports for enzyme immobilization have been done. Structure and morphology of prepared new materials were characterized by attenuated total reflectance Fourier-transform infrared (ATR-FTIR), XRD, and TEM analysis. Next, the immobilization of lipase from *Candida rugosa* was performed on the nanoparticles surface via *N*-(3-dimethylaminopropyl)-*N*'-ethylcarbodiimide hydrochloride (EDC)/*N*-hydroxy-succinimide (NHS) mechanism. The best results of lipase activity recovery and specific activities were observed for nanoparticles with polymer shell crosslinked via a novel procedure with squaric acid. The specific activity for lipase immobilized on materials crosslinked with SqA (52 U/mg lipase) was about 2-fold higher than for enzyme immobilized on MNPs with glutaraldehyde addition (26 U/mg lipase). Moreover, a little hyperactivation of lipase immobilized on nanoparticles with SqA was observed (104% and 112%).

**Keywords:** immobilization; lipase; magnetic nanoparticles; chitosan; collagen; squaric acid

## 1. Introduction

Lipases are one of the most used hydrolases, and are applied in wide range of organic reactions as well as in analytical procedures [1,2]. The active center of the lipases from *Candida rugosa* is covered by a polypeptide chain called lid. This polypeptide can rearrange and consequently leads to conformational changes of lipases at the interface of water and organic phases. As a result of this rearrangement near the lipase active center, a significant increase of enzyme activity is observed [3–6]. Free form of lipase has a poor stability and it is not possible to use this enzyme in several catalytic cycles. Moreover, the separation of enzyme after reaction is somewhat complicated and needs centrifugation and precipitation. One of the most promising methods to improve the enzyme's disadvantages is immobilization [7,8]. The strategy of immobilization has a great impact on the attached enzyme properties—it may improve enzyme activity, stability, selectivity, and specificity [9,10]. In general,

a reversible method could be more advantageous, but there is no universal strategy for enzyme immobilization, and it will depend on many factors, especially on enzyme limitation properties. Immobilization of enzymes may lead to various changes in enzyme properties: it may promote a diffusion problem, block the enzyme active center, and cause enzyme distortion [11]. The use of nonporous nanomaterials as a support seems to be a possible solution of these issues. The enzyme immobilized on nonporous nanomaterial is usually properly oriented, without diffusion problems, and consequently could be characterized by good enzyme activity and stability [9]. It has been reported that enzyme stability may be also improved if an intense multipoint covalent binding between an enzyme molecule and a rigid support is obtained [12,13]. The rapidly growing field of enzymatic reactions in biotechnology needs new supports for immobilizations that guarantee simple catalytic system separation and high reusability. Usually, the binding of bioligands (such as enzymes) is accomplished through surface adsorption, covalent bonding, and encapsulation. For enzymes, there are two ways for effective immobilization: physical adsorption and chemical immobilization using the covalent bonds between reactive groups of the enzyme and the support surface. Among the physical adsorption mechanisms, covalent immobilization seems to be more effective for enzymes due to the stabilization of their active conformation [14].

Magnetic nanoparticles (MNPs) are widely used as supports for physical and chemical biomolecule immobilization [15–17], with usually a high load of ligands [18–21]. However, pure magnetite has a poor colloidal stability, particularly in neutral pH, so it needs stabilization and surface modification [22]. Although MNPs generally are appropriate supports for biocatalysis, especially in industrial applications, some types of these material—especially when coated with silica compounds—may show some disadvantages [9]. After successful use of dextran for MNP surface stabilization, polymers are most frequently used for such particle-coating. Polymer shells for MNPs give the possibility of controlling the composition of the material's surface [23]. A polymer shell coated on a magnetic core needs structure stabilization by crosslinking. Glutaraldehyde (Glu) (Figure 1a) and epichlorohydrine were usually used as crosslinkers for chitosan. For collagen materials, many crosslinkers were tested (e.g., dialdehydes, isocyanates, and carbodiimides), but they are often “not friendly” for biomedical applications and can interact with bioligands, reducing the effectivity of immobilization [24,25].

Squaric acid (3,4-dihydroxy-3-cyclobutene-1,2-dione, SqA) is a planar, cyclic structure able to interact with amino groups in a simple condensation reaction (Figure 1b). Moreover, it seems to work better in biomedical applications, as it is nontoxic and less aggressive to biomolecules than glutaraldehyde, for example [26]. In our previous study, hydrogels obtained by crosslinking a mixture of two proteins, collagen/elastin, for tissue engineering have been successfully prepared with a squaric acid addition [27]. The *in vitro* tests show that SqA would be a safe and effective protein crosslinker instead of the popular glutaraldehyde or epichlorohydrine.

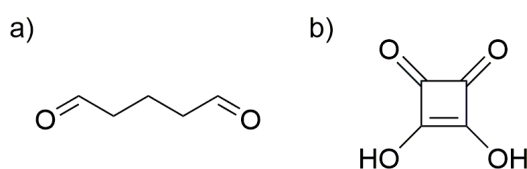


**Figure 1.** Structures of applied crosslinking agents (a) glutaraldehyde (Glu); (b) squaric acid (SqA).

Herein, the use of SqA as a safe crosslinker for polysaccharide and a mixture of polysaccharide and protein was examined. The syntheses of six types of chitosan (CS)-, collagen (Coll)-, and CS/Coll-coated magnetic nanoparticles were done. Although chitosan-coated MNPs crosslinked with Glu and epichlorohydrine are well described, the crosslinking of polysaccharides with SqA was not reported, especially on MNP surfaces. The use of collagen as a polymer shell for MNPs was also not reported in literature. In this work, the polymer layer coated on MNPs was crosslinked traditionally with Glu

and with SqA as a new crosslinking agent. Four types of prepared nanoparticles are novel. All of the prepared magnetic nanomaterials were used for covalent immobilization of lipase from *Candida rugosa* via *N*-(3-dimethylaminopropyl)-*N'*-ethylcarbodiimide hydrochloride (EDC)/*N*-hydroxy-succinimide (NHS) lipase activation procedure. Nanoparticles were characterized by analytical methods: attenuated total reflectance Fourier-transform infrared (ATR-FTIR), XRD, and TEM. The activity, reusability, and the amount of lipase immobilized on MNPs' surface were determined, and the effect of crosslinker on material stability and enzyme activity was investigated.

## 2. Results and Discussion

### 2.1. Magnetic Nanoparticles Synthesis and Characterization

Six types of MNPs coated with chitosan, collagen, and the blend of these two biopolymers were prepared by standard coprecipitation reaction. This route of synthesis was feasible due to the good solubility of the biopolymers in acidic conditions and precipitation at a pH of about 12. Collagen used for nanoparticle-coating was isolated from the tail tendons of young rats according to literature procedure [28]. A commercially available collagen has been also used, and no differences between these two types of protein were observed. For magnetic nanoparticle-coating, the biopolymers CS and Coll were used alone or in 1:1 weight ratio. Two types of crosslinkers were used for polymer layer stabilization: glutaraldehyde (Glu) and squaric acid (SqA) (Figure 1). Finally, CS/Glu ( $\text{Fe}_3\text{O}_4$ ), Coll/Glu ( $\text{Fe}_3\text{O}_4$ ), CS–Coll/Glu ( $\text{Fe}_3\text{O}_4$ ), Coll/SqA ( $\text{Fe}_3\text{O}_4$ ), CS/SqA ( $\text{Fe}_3\text{O}_4$ ), and CS–Coll/SqA ( $\text{Fe}_3\text{O}_4$ ) nanoparticles were obtained. Due to the presence of primary amino groups in CS and Coll structures, the crosslinking reaction with carbonyl groups of Glu and SqA was possible to perform, and the use of SqA as a virgin polysaccharide and the mixture component crosslinker was not reported (Figure 2) [27]. Although the primary amino groups in polymers reacted with crosslinkers, the surface of all prepared nanoparticles was still rich in these groups and able to bond bioligands. The amount of  $\text{NH}_2$  groups was determined by standard ninhydrin method [29] and varied between 2.05 mM/g for CS–Coll/Glu ( $\text{Fe}_3\text{O}_4$ ) and 3.73 mM/g for CS/Glu ( $\text{Fe}_3\text{O}_4$ ) as it is shown in Table 1.

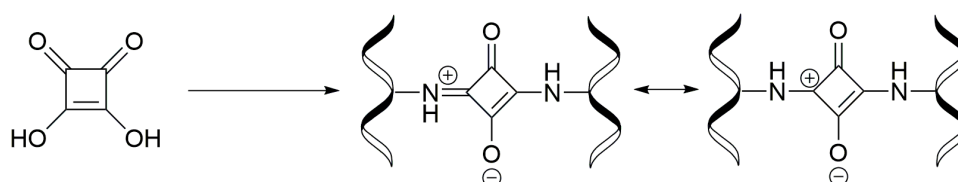


Figure 2. Scheme of collagen and chitosan crosslinking with squaric acid (SqA).

Table 1. Characteristic of prepared nanoparticles surface <sup>1</sup>.

Nanoparticles Type	Size (nm)	Amount of $\text{NH}_2$ Groups (mM/g)
CS/Glu ( $\text{Fe}_3\text{O}_4$ )	16	3.73
CS/SqA ( $\text{Fe}_3\text{O}_4$ )	20	3.31
Coll/Glu ( $\text{Fe}_3\text{O}_4$ )	21	3.51
Coll/SqA ( $\text{Fe}_3\text{O}_4$ )	29	2.17
CS–Coll/Glu ( $\text{Fe}_3\text{O}_4$ )	24	2.05
CS–Coll/SqA ( $\text{Fe}_3\text{O}_4$ )	32	2.83

<sup>1</sup> CS: chitosan, Coll: collagen.

The size of prepared nanoparticles was investigated using zeta sizer (Table 1). The average size varies between 16 and 32 nm. The dynamic light scattering (DLS) analysis also demonstrated that prepared nanoparticles are rather homogenous in size. These observations were validated by conventional TEM analysis, which demonstrated that particles are aggregate with medium size (20–30 nm) for a particle (Figure 3) and, in all cases, were a little bigger when SqA was used.

To determine the structure of the magnetic core, electron diffraction was applied. The typical selected area diffraction pattern (SADP) for the studied group of particles is shown in Figure 3.

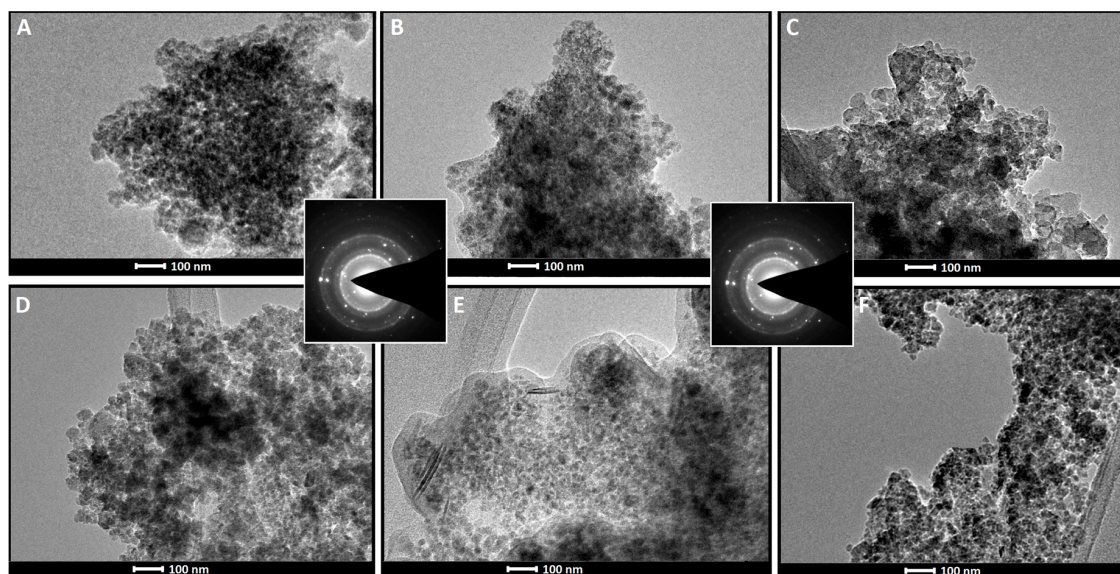


**Figure 3.** TEM images of (A) Coll/Glu ( $\text{Fe}_3\text{O}_4$ ); (B) CS-Coll/Glu ( $\text{Fe}_3\text{O}_4$ ); (C) CS/Glu ( $\text{Fe}_3\text{O}_4$ ); (D) Coll/SqA ( $\text{Fe}_3\text{O}_4$ ); (E) CS-Coll/SqA ( $\text{Fe}_3\text{O}_4$ ); (F) CS/SqA ( $\text{Fe}_3\text{O}_4$ ) nanoparticles.

The structure of the magnetic nanoparticles was characterized by ATR-FTIR spectroscopy (Figure 4) and compared with the spectrum of pure CS and Coll. The spectrum of nanoparticles coated only with chitosan shows characteristic broad peak at  $3460\text{--}3264\text{ cm}^{-1}$  from the stretching vibrations of OH and  $\text{NH}_2$  groups. It should be added that the stretching vibrations of  $\text{NH}_2$  group of chitosan were masked by the OH group peak. The vibration peak at  $1647\text{--}1636\text{ cm}^{-1}$  increased with the C=N groups formation as a result of glutaraldehyde or squaric acid crosslinking reaction. Collagen displayed bands at  $1630$ ,  $1550$ , and  $1220\text{ cm}^{-1}$ , characteristic for the amide I, II, and III groups. The broad absorption band was observed at  $3307\text{ cm}^{-1}$ , assigned to the stretching vibration of N-H groups from the collagen macromolecule. The spectra of the Coll/Glu ( $\text{Fe}_3\text{O}_4$ ) and the Coll/SqA ( $\text{Fe}_3\text{O}_4$ ) also showed bands at  $3360\text{ cm}^{-1}$  (N-H) and  $1630\text{ cm}^{-1}$  (amide C=O stretching vibration). Bands at  $2940$  and  $1010\text{ cm}^{-1}$  indicated the aliphatic CH, and bending vibrations of CO, respectively. All of these characteristic bands were observed in CS-Coll/Glu ( $\text{Fe}_3\text{O}_4$ ) and the CS-Coll/SqA ( $\text{Fe}_3\text{O}_4$ ) spectra. In all spectra of nanoparticles with SqA as a crosslinker, characteristic bands at  $1370\text{ cm}^{-1}$  (CS-Coll/SqA ( $\text{Fe}_3\text{O}_4$ )),  $1356\text{ cm}^{-1}$  (Coll/SqA ( $\text{Fe}_3\text{O}_4$ )), and  $1438\text{ cm}^{-1}$  (CS/SqA ( $\text{Fe}_3\text{O}_4$ )) were observed. These bands were assigned to the  $-\text{OH}(-\text{O}^-)$  bending vibrations from the squaric moiety. The Fe-O group of magnetite showed a signal at  $595\text{ cm}^{-1}$ , which was observed in spectra of all the nanoparticles. The crystal structure and phase purity of prepared nanoparticles were also verified by XRD analysis. The patterns exhibit diffraction peaks which were indexed as (2 2 0), (3 1 1), (4 0 0), (4 2 2), (5 1 1), and (4 4 0) reflections, characteristics of the spinel structure of  $\text{Fe}_3\text{O}_4$ . These peaks are in accordance with the X'Pert High Score database. This results demonstrated that the presence of collagen and chitosan coats on the surface of  $\text{Fe}_3\text{O}_4$  did not lead to a phase change.

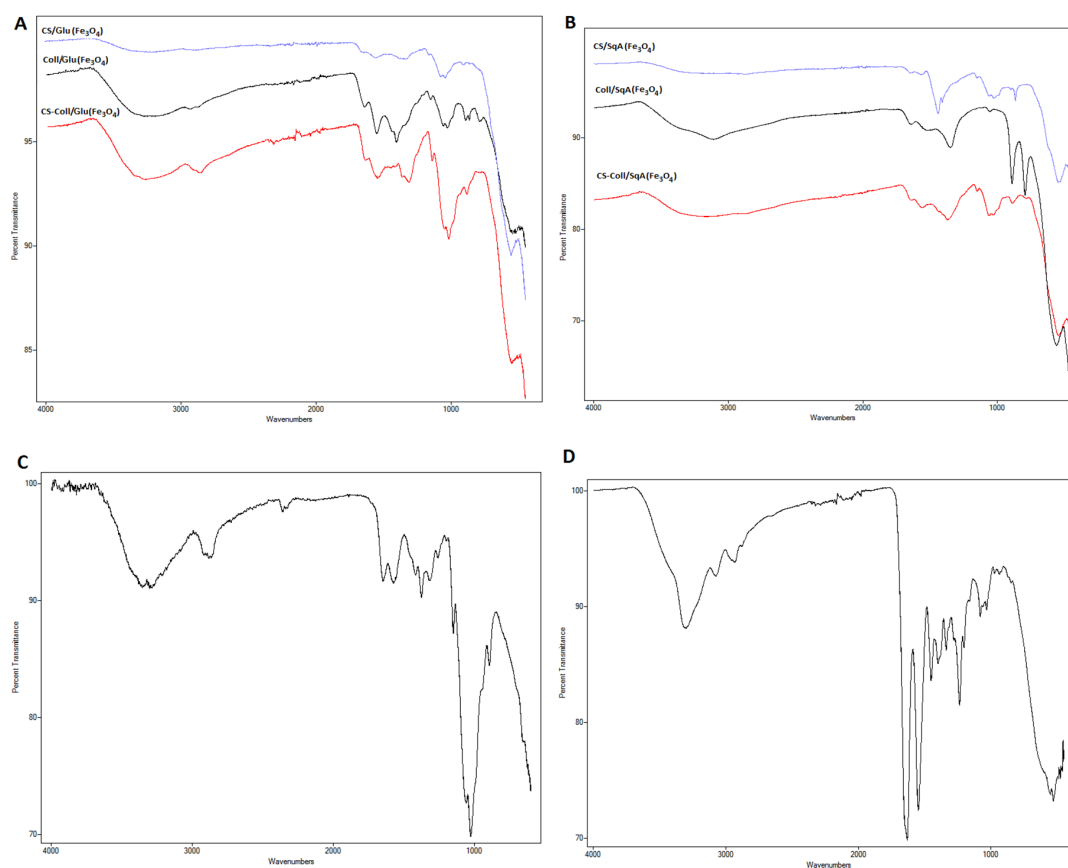


**Figure 4.** Attenuated total reflectance Fourier-transform infrared (ATR-FTIR) spectra of the obtained nanoparticles (A,B), pure chitosan (C), and collagen (D).

## 2.2. Immobilization of Lipase from *Candida rugosa*

Lipase from *Candida rugosa* was covalently immobilized on all prepared nanoparticle surfaces. The immobilization took place via standard EDC/NHS procedure, using NH<sub>2</sub> groups of the support and carboxylic groups of the enzyme (Figure 5) [15]. Lipase carboxylic groups were firstly activated with EDC and NHS and then reacted with amino groups of the magnetic support. The optimization of the lipase immobilization procedure was previously reported and applied in this work [30].

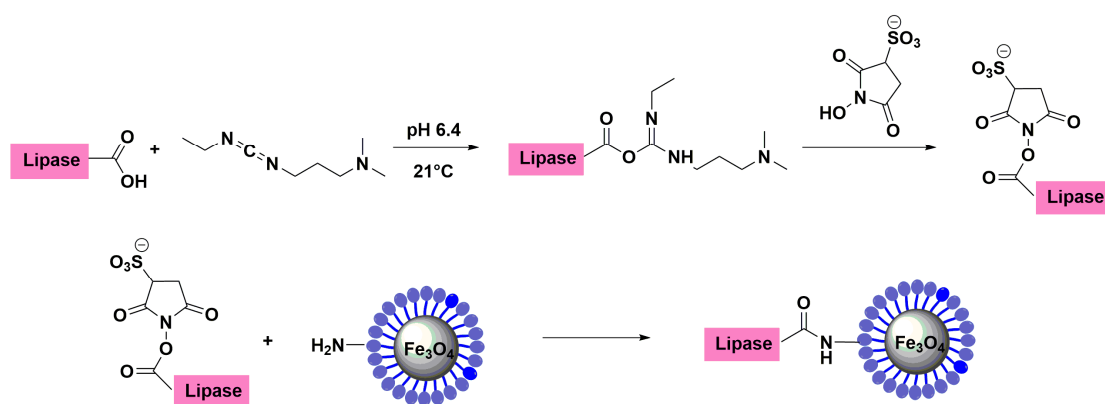


**Figure 5.** Scheme of lipase immobilization on magnetic nanoparticles (MNPs).

The amount of immobilized lipase bonded on the magnetic nanoparticles surface was investigated as the difference between the initial and final concentration of enzyme following the Bradford method

(Table 2) [31]. As it is shown, the high lipase loading was observed for nanoparticles coated with the mixture of chitosan and collagen crosslinked traditionally with Glu. The crosslinked collagen coated on the surfaces of nanoparticles did not distort the Bradford test quality—collagen needs to be treated with 6 M HCl under reflux to be detectable in this method [32]. In all cases, crosslinking the polymeric shell with squaric acid (SqA) reduced the amount of immobilized lipase on the support surface.

**Table 2.** Lipase from *Candida rugosa* immobilization results.

Nanoparticles Type	Lipase Loading (mg/g)	Activity Recovery (%)	Lipase Activity (U)	Hydrolytic Activity (U/g Support)	Specific Activity (U/mg Lipase)
CS/Glu (Fe <sub>3</sub> O <sub>4</sub> )	67	77	85.3	1706	25.5
CS/SqA (Fe <sub>3</sub> O <sub>4</sub> )	47	104	70.5	1410	30
Coll/Glu (Fe <sub>3</sub> O <sub>4</sub> )	63	85	82.1	1642	26
Coll/SqA (Fe <sub>3</sub> O <sub>4</sub> )	18	97	47	940	52.2
CS–Coll/Glu (Fe <sub>3</sub> O <sub>4</sub> )	74	94	90.7	1814	24.5
CS–Coll/SqA (Fe <sub>3</sub> O <sub>4</sub> )	27	112	60.1	1202	44.5

### 2.2.1. Lipase Activity and Recovery

The effect of polymer shell crosslinking on lipase activity and stability was investigated. As it is shown, the immobilization efficiency was lower for nanoparticles prepared with squaric acid as a crosslinking agent, but quite different results were observed for lipase activity (Table 2).

Although the amount of immobilized lipase was rather low for nanosupports with squaric acid addition as a polymer crosslinker, the activity recovery of immobilized enzyme increased for these materials. When glutaraldehyde as crosslinker was applied, the activity recovery of immobilized lipase was about 77%–85% for nanoparticles coated with virgin CS or Coll, and a little higher—about 94%—for nanoparticles coated with a mixture of these two biopolymers. Lipases immobilized onto materials crosslinked with squaric acid were characterized by better activity recovery in all types of support. The activity recovery was about 97% for nanoparticles coated with Coll, and higher than 100% for two other materials: CS/SqA (Fe<sub>3</sub>O<sub>4</sub>) and CS–Coll/SqA (Fe<sub>3</sub>O<sub>4</sub>). The specific activities of lipase immobilized on all supports with SqA polymer shell crosslinking were also higher than for these same materials crosslinked with Glu. The best results for enzyme specific activity were observed for nanoparticles coated with collagen crosslinked with SqA—about 2-fold better than for material where Glu was applied as a collagen crosslinker. It is known in literature that air bubbles and other proteins could stabilize the soluble enzymes and consequently improved their catalytic activity [33]. In this case, a small hyperactivation of immobilized enzyme was observed. Moreover, the crosslinking of collagen or chitosan with squaric acid in a condensation reaction led to ionic structure as it is shown in Figure 2. It was reported that very low concentration of ionic compounds made lipases in solution dramatically hyperactivated (above 300-fold) [34,35]. The ionic form of the squaric moiety in a crosslinked polymer shell may promote activation and stabilization of the open form of lipase, and, finally, the hyperactivity was observed.

These results of enzyme activities are only a model to show the potential of new magnetic nanoparticles synthesized without Glu as a friendly support for biocatalysis. In the future, the multipoint immobilization and usage of other activators like epoxides or divinylsulphones will be of general interest.

### 2.2.2. Immobilized Lipase Stability—Optimal pH and Temperature

To find the optimal pH value and temperature with maximum hydrolytic activity of the immobilized lipase, the influence of different pH values and temperatures were applied and the activity recovery of free and immobilized lipase was investigated.

The pH effect of the free and immobilized lipase was investigated by enzyme incubation in the mixture of emulsion (gum arabic and olive oil) and the buffer solution (100 mM, pH 4–10). The analysis using a standard activity assay procedure as well as determination of the relative activity were

performed (relative activity (%)) is the ratio between activity of every sample and the maximum sample activity). As it is shown in Figure 6, the optimal pH of free and immobilized lipase of all of prepared supports is 7. For pH values lower than optimal 7, the lipase immobilized on CS–Coll/SqA ( $\text{Fe}_3\text{O}_4$ ) nanoparticles was more stable (about 75% of relative activity) compared to the native form of enzyme (60%). The differences were more significant in pH values between 9 and 10. All prepared nanoparticles showed about 70%–80% of relative activity at pH = 9 and 58%–70% at pH 10, whereas the native form of lipase remained at only 50% of activity at pH 9 and 20% of activity at pH 10. Therefore, the process of immobilization increased the relative activities of enzyme by an average of 1.5- and 3.2-times at pH = 9 and pH = 10, respectively, compared to the results obtained with the native form of enzyme. By comparison, Shang et al. described the immobilization of *Candida rugosa* lipase (CRL) via adsorption on ZnO nanowires/macroporous silica composites [36]. The native form of lipase retained about 40% and 21% relative activity of triacetin hydrolysis reaction at pH 9 and pH 10, whereas at the same pH conditions, immobilized CRL retained 89.9% and 80.2% relative activity, respectively.

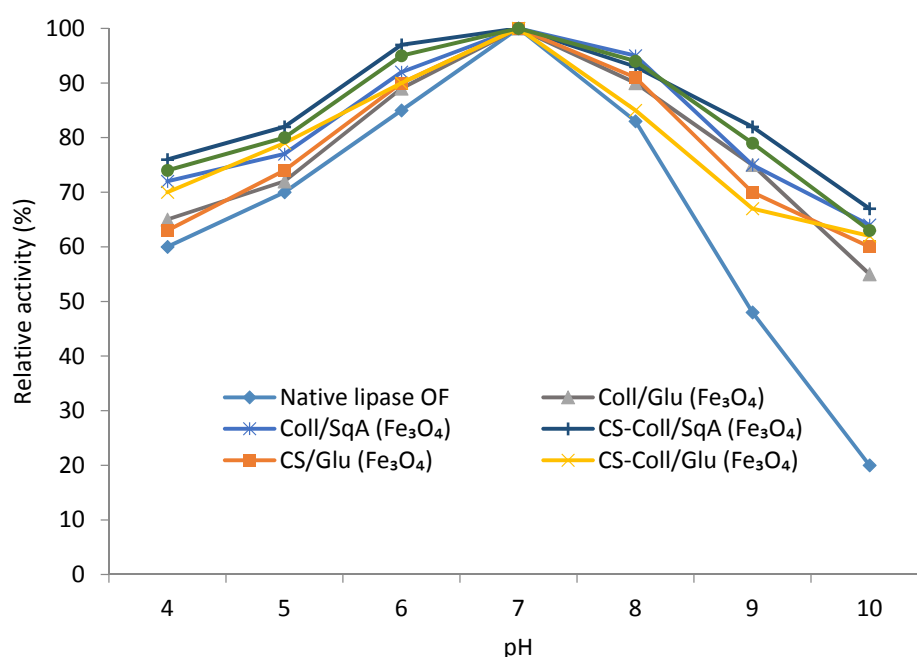
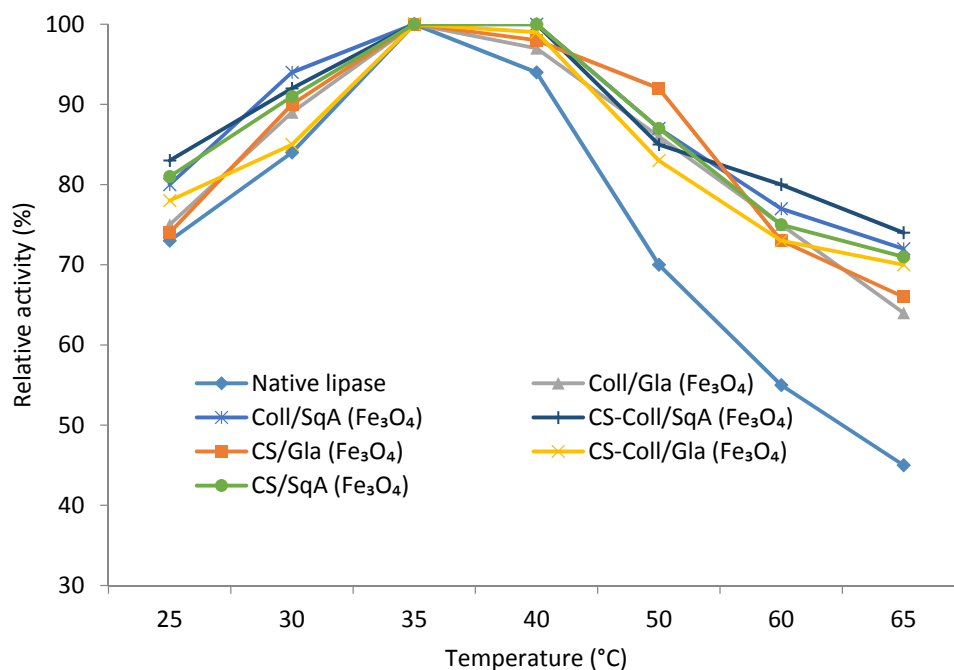


Figure 6. Effect of pH value on lipase activity.

The effect of temperature on lipase activity and stability was performed in phosphate buffer (pH 7.4) and temperature range from 25 to 65 °C for 30 min with the use of emulsion of gum arabic and olive oil (standard activity assay). The relative activities were determined and are presented in Figure 7.

The optimal temperature of lipase immobilized on all supports was about 35–40 °C and it is similar to the optimal temperature for native lipase (35 °C). The lipase immobilized on MNPs with a polymer shell crosslinked with squaric acid was the most stable (the relative activity was 100% in the range of 35–40 °C). The relative activity of immobilized lipase at higher temperatures (50–65 °C) was about 75%, while the activity of free lipase decreased to 50%–45%. In this case, the most stable was lipase immobilized on CS–Coll/SqA ( $\text{Fe}_3\text{O}_4$ ) and Coll/SqA ( $\text{Fe}_3\text{O}_4$ ) nanoparticles. At 60 °C, all prepared nanoparticles remained at 72%–83% relative activity and about 67%–75% at 65 °C, while free lipase showed about 55% and 45% relative activity at 60 and 65 °C, respectively. Hou et al. prepared core–shell magnetic polydopamine/alginate biocomposite for covalent immobilization of lipase from *Candida rugosa*. The effect of temperature of immobilized-lipase support was based also on the hydrolysis of olive oil. Compared with free lipase, the immobilized enzyme kept its relative

activity up to about 85% at the temperature of 60 °C, while free lipase exhibited about 60% in the same temperature [37]. Mahto et al. immobilized *Candida rugosa* lipase via electrostatic adsorption on magnetic mesoporous silica nanocomposites with polyaniline moieties [38]. The immobilized lipase demonstrated about 77% of its relative activity at 60 °C of *p*-nitrophenyl butyrate (pNPB) hydrolysis reaction, however, free lipase retained about 50% of relative activity. What should be stressed is that the immobilized enzyme is more resistant to temperature changes compared to the native form of lipase. The relative activity was higher for bound biocatalyst compared to free form at all ranges of tested temperatures ( $T = 25\text{--}65$  °C).



**Figure 7.** Effect of temperature on lipase activity.

### 2.2.3. Reusability of Immobilized Lipase

To examine the operational stability of the immobilized enzyme, lipase immobilized onto magnetic nanoparticles was reused to catalyze the hydrolysis of the olive oil. The reusability of the immobilized lipase was investigated for 10 consecutive cycles. As it is shown in Figure 8, after 5th use, the residual activities for all studied magnetic nanoparticles were about 80%–90%, and at the end of the 10th use, immobilized lipases still retained almost 80% of their activities, depending on the support applied. In Hou et al.'s work [37], the residual activity of lipase immobilized on core–shell magnetic polydopamine/alginate biocomposite, based on the hydrolysis of olive oil, was about 82% and 77% after the 10th and 12th cycles of reaction, respectively. In Wang et al.'s article, the lipase from *Candida rugosa* was immobilized on magnetite nanoparticles with three-dimensional graphene oxide–chitosan composites by one of three methods: electrostatic adsorption, metal-ion affinity interactions, or covalent bonding [39]. The residual activity of immobilized lipase based on the results of hydrolysis of olive oil was about 63%–70% after 10 reaction cycles, depending on the applied immobilization methods. These results are comparable with results presented in this article.



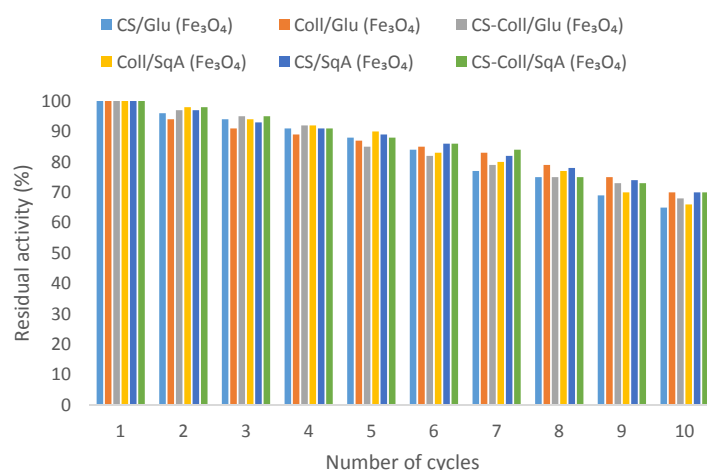


Figure 8. Reusability of lipase immobilized on magnetic nanoparticles.

### 3. Materials and Methods

#### 3.1. Materials

Iron (II) chloride tetrahydrate, iron (III) chloride hexahydrate, chitosan (low molecular weight), glutaraldehyde, squaric acid, acetic acid, sodium hydroxide, EDC (*N*-(3-dimethylaminopropyl)-*N*'-ethylcarbodiimide hydrochloride), sulfo-NHS (*N*-hydroxy-sulfosuccinimide sodium salt), glycine, olive oil, ninhydrin reagent, and Bradford reagent were purchased from Sigma-Aldrich (Darmstadt, Germany) and used without further purification. Solvents, sodium phosphate dibasic dihydrate, and orthophosphoric acid solution, sodium acetate, and gum arabic were purchased from POCH Gliwice (Gliwice, Poland). All solutions were prepared with deionized water. Lipase OF from *Candida rugosa* (activity 380,000 U/g powder) was a gift from Meito Sangyo Co., Ltd. (Nagoya, Japan). Experiments with air- and moisture-sensitive materials were carried out under nitrogen atmosphere. Glassware was oven-dried for several hours, assembled hot, and cooled in a stream of nitrogen.

#### 3.2. Isolation of Collagen from Rats Tail Tendons

After washing with distilled water, the rat tendons were dipped in acetic acid solution (0.1 M) for 4 days at 4 °C. Collagen dissolved in acetic acid was freeze-dried (48 h, −20 °C, 100 Pa) to obtain pure protein.

#### 3.3. Synthesis of Collagen-Coated Nanoparticles Crosslinked with Glutaraldehyde Coll/Glu (Fe<sub>3</sub>O<sub>4</sub>)

Collagen from rat tails (0.2 g, local source) was added into 1% acetic acid solution (20 mL) and mechanically stirred at room temperature until solution become homogenous. Iron (II) chloride tetrahydrate (3.7 mmol), iron (III) chloride hexahydrate (7.5 mmol) were added. Slow addition of droplets of 30% solution of NaOH (15 mL) formed magnetic nanoparticles. The resulting nanomaterial was filtrated and thoroughly washed with deionized water five times. Then, 20 mL of 6.5% glutaraldehyde/water solution was added, and the mixture was mechanically stirred at room temperature for 30 min. The obtained magnetic material was magnetically separated, thoroughly washed with deionized water, and finally dried under vacuum at 50 °C for 24 h.

#### 3.4. Synthesis of Collagen-Coated Nanoparticles Crosslinked with Squaric Acid Coll/SqA (Fe<sub>3</sub>O<sub>4</sub>)

Collagen from rat tails (0.2 g, local source) was added into 1% acetic acid solution (20 mL) and mechanically stirred at room temperature until solution become homogenous. Iron (II) chloride tetrahydrate (3.7 mmol), iron (III) chloride hexahydrate (7.5 mmol) were added. Slow addition of droplets of 30% solution of NaOH (15 mL) formed magnetic nanoparticles. The resulting nanomaterial

was filtrated and thoroughly washed with deionized water five times. Then, squaric acid (0.022 g, 0.2 mmol) in ethanol (100 mL) was added and the blend was magnetically stirred at 30 °C for 2 h. The obtained magnetic material was magnetically separated, thoroughly washed with deionized water, and finally dried under vacuum at 50 °C for 24 h.

### 3.5. Synthesis of Chitosan-Coated Nanoparticles Crosslinked with Glutaraldehyde CS/Glu ( $Fe_3O_4$ )

The procedure for Coll/Glu ( $Fe_3O_4$ ) was used with 0.2 g of chitosan.

### 3.6. Synthesis of Chitosan-Coated Nanoparticles Crosslinked with Squaric Acid CS/SqA ( $Fe_3O_4$ )

The procedure for Coll/SqA ( $Fe_3O_4$ ) was used with 0.2 g of chitosan.

### 3.7. Synthesis of Chitosan–Collagen (1:1) Coated Nanoparticles Crosslinked with Glutaraldehyde CS–Coll/Glu ( $Fe_3O_4$ )

Collagen from rat tails (0.1 g, local source) and chitosan (0.1 g) were added into 1% acetic acid solution (20 mL) and mechanically stirred at room temperature until solution become homogenous. Iron (II) chloride tetrahydrate (3.7 mmol) and iron (III) chloride hexahydrate (7.5 mmol) were added. Slow addition of droplets of 30% solution of NaOH (15 mL) formed magnetic nanoparticles. The resulting nanomaterial was filtrated and thoroughly washed with deionized water five times. Then, 20 mL of 6.5% glutaraldehyde/water solution was added and the mixture was mechanically stirred at room temperature for 30 min. The obtained magnetic material was magnetically separated, washed with deionized water, and finally dried under vacuum at 50 °C for 24 h.

### 3.8. Synthesis of Chitosan–Collagen (1:1) Coated Nanoparticles Crosslinked with Squaric Acid CS–Coll/SqA ( $Fe_3O_4$ )

Collagen from rat tails (0.1 g, local source) and chitosan (0.1 g) were added into 1% acetic acid solution (20 mL) and mechanically stirred at room temperature until solution become homogenous. Iron (II) chloride tetrahydrate (3.7 mmol) and iron (III) chloride hexahydrate (7.5 mmol) were added. Slow addition of droplets of 30% solution of NaOH (15 mL) formed magnetic nanoparticles. The resulting nanomaterial was filtrated and thoroughly washed with deionized water five times. Then, squaric acid (0.022 g, 0.2 mmol) in ethanol (100 mL) was added and the blend was magnetically stirred at 30 °C for 2 h. The obtained magnetic material was magnetically separated, washed with deionized water, and finally dried under vacuum at 50 °C for 24 h.

### 3.9. Quantification of Available Primary Amino Groups on Magnetic Nanoparticles Surface

The amount of primary amino groups on prepared magnetic MNPs was investigated by the standard ninhydrin method. The calibration curve was performed using glycine as a standard—ranging from 0.6 to 2 mM in 0.1 mM acetate buffer, pH 5.5 (0.5 g of ninhydrin was dissolved in a solution of 30 mL of isopropanol and 20 mL of acetate buffer to prepared solution). Freshly prepared ninhydrin reagent (2 mL) was added to 2 mL solution of each concentration of glycine and was then well mixed. The blank reagent consisted of 2 mL of distilled water and 2 mL of freshly prepared ninhydrin reagent. Each of synthesized nanoparticles were dispersed in 2 mL of 0.1 mL buffer acetate (pH 5.5) and then 2 mL of ninhydrin reagent was added. The tubes were immediately capped, shaken by hand and heated in boiling water bath for 15 min. The tubes were then cooled and the content diluted with 3 mL of 50% ethanol solution. The concentration of primary amino groups was measured at 570 nm in the UV spectrophotometer (UV-1800, Shimadzu, Kyoto, Japan).

### 3.10. Immobilization of Lipase from *Candida rugosa* onto MNPs Surface

Fifty microliters of EDC solution (2 mg/50  $\mu$ L phosphate buffer) was added to the tube containing 36.6 mg of lipase OF dissolved in 1 mL phosphate buffer and placed at 21 °C in a thermomixer for 1 h. Next, 50  $\mu$ L of sulfo-NHS solution (2.4 mg/50  $\mu$ L phosphate buffer) was added to the above

reaction solution and the incubation was continued for 1 h. The prepared solution was transferred into a new tube containing the previously rinsed magnetic nanoparticles with 50 mM phosphate buffer and the incubation continued for 2 h. Nanoparticles with the immobilized lipase were rinsed a few times with 0.5 mL of deionized water and dried overnight at 30 °C. The amount of immobilized lipase bonded on the magnetic nanoparticles surface was determined as the difference between the initial and final concentration of enzyme following to the Bradford method. A calibration curve constructed with lipase OF solution of known concentration (0.5–2 mg/mL) was used in the calculation of enzyme concentrations. All data used for calculation are average of triplicate of the experiments.

### 3.11. Assay of Immobilized Lipase Activity

The activity of free and immobilized lipase was measured by titration of the fatty acid obtained through the hydrolysis of the olive oil. A 100 mL olive oil emulsion was prepared by mixing of olive oil (50 mL) and gum arabic solution (50 mL, 7% *w/v*). The assay mixture consisted of the emulsion (5 mL), phosphate buffer (2 mL, 100 mM, pH 7.4) and either free enzyme (1 mL) or immobilized lipase (50 mg nanoparticles in 1 mL buffer). Oil hydrolysis was performed at 37 °C for 30 min. in a shaking water bath at 150 rpm. The reaction was stopped by the addition of 10 mL of ethanol-acetone solution (1:1). The amount of the liberated fatty acid in the medium was determined by the titration with 50 mM NaOH solution using phenolphthalein as indicator. One unit of lipase activity (U) was defined as the amount of the enzyme required to hydrolyze olive oil that caused release of 1 μM of fatty acid per minute under the assay condition. Activity recovery (%) was the ratio between the activity of immobilized lipase and the activity of the equal amount of the free lipase in solution.

### 3.12. Operational Stability (Reusability) of Lipase Immobilized onto MNPs

To examine the operational stability of the immobilized enzyme, lipase immobilized onto magnetic nanoparticles was reused to catalyze the hydrolysis of the olive oil. Magnetic nanoparticles with lipase after a catalytic cycle were washed three times with the phosphate buffer (2 mL, 100 mM, pH 7.4) and next mixed with the freshly prepared reaction mixture to start a new cycle. The immobilized enzyme was reused 10 times. The residual activity (%) was estimated as the ratio between the activity of the immobilized lipase in the *n*th cycle and the activity of immobilized lipase in the 1st cycle, where the activity of the 1st cycle is defined as 100%. All obtained values were expressed in percentage.

## 4. Conclusions

Six types of magnetic nanoparticles coated with two biopolymers, chitosan and collagen, were synthesized (four of them were novel). Squaric acid (SqA) as a nontoxic crosslinking agent was applied for polymeric shell stabilization and compared with glutaraldehyde (Glu), a widely used crosslinker. Lipase from *Candida rugosa* was immobilized onto all prepared nanoparticles and the activity, reusability, and thermal stability were investigated. Enzymes immobilized onto MNPs with polymer shell crosslinked with SqA were characterized with better activity than enzymes immobilized onto MNPs using Glu. The specific activity of lipase immobilized on MNPs with surface crosslinking using SqA was about 2-fold higher than for MNPs with Glu addition. Moreover, the lipase hyperactivation was observed on materials that contained collagen and that were crosslinked with SqA. The lipase thermal and pH stabilities were also better for materials with SqA addition.

In summary, squaric acid (SqA) is a safe, “enzyme friendly” crosslinking agent, which could be successfully applied for polymer crosslinking in any type of support designed for enzyme immobilization or encapsulation. Furthermore, this strategy for virgin and MNP surface-coated polysaccharides and proteins crosslinked with SqA could be extended to other materials based on these biopolymers.

**Acknowledgments:** This work was supported by the National Science Centre Poland grant 2014/15/D/NZ7/01805 and partially (enzymatic part) by the NSC (National Science Centre Poland) grant 2014/15/B/NZ7/00972. All publication costs in Catalysts were supported by 2014/15/D/NZ7/01805 grant.

**Author Contributions:** Marta Ziegler-Borowska conceived and designed the experiments, partially performed the experiments, analyzed the data, contributed reagents/materials/analysis tools and wrote the paper; Dorota Chelminiak-Dudkiewicz and Katarzyna Wegrzynowska-Drzymalska performed the nanoparticles synthesis and IR analysis. Adam Sikora, Tomasz Siódmiak and Michał P. Marszał performed the enzyme immobilization. Joanna Skopinska-Wisniewska isolated the collagen from rat tails. Halina Kaczmarek partially analyzed the data.

**Conflicts of Interest:** The authors declare no conflict of interest. The founding sponsors had no role in the design of the study; in the collection, analyses, or interpretation of data; in the writing of the manuscript, and in the decision to publish the results.

## References

1. Siódmiak, T.; Mangelings, D.; Heyden, Y.V.; Ziegler-Borowska, M.; Marszał, M.P. High enantioselective novozym 435-catalyzed esterification of (*R,S*)-flurbiprofen monitored with a chiral stationary phase. *Appl. Biochem. Biotechnol.* **2015**, *175*, 2769–2785. [[CrossRef](#)] [[PubMed](#)]
2. Rivero, C.; Palomo, J. Covalent immobilization of *Candida rugosa* lipase at alkaline pH and their application in the regioselective deprotection of per-*O*-acetylated thymidine. *Catalysts* **2016**, *6*, 115. [[CrossRef](#)]
3. Grochulski, P.; Li, Y.; Schrag, J.D.; Bouthillier, F.; Smith, P.; Harrison, D.; Rubin, B.; Cygler, M. Insights into interfacial activation from an open structure of *Candida rugosa* lipase. *J. Biol. Chem.* **1993**, *268*, 12843–12847. [[PubMed](#)]
4. Grochulski, P.; Li, Y.; Schrag, J.D.; Cygler, M. Two conformational states of *Candida rugosa* lipase. *Protein Sci.* **1994**, *3*, 82–91. [[CrossRef](#)] [[PubMed](#)]
5. De Domínguez María, P.; Sánchez-Montero, J.M.; Sinisterra, J.V.; Alcántara, A.R. Understanding *Candida rugosa* lipases: An overview. *Biotechnol. Adv.* **2006**, *24*, 180–196. [[CrossRef](#)] [[PubMed](#)]
6. De Albuquerque, T.L.; Rueda, N.; dos Santos, J.C.S.; Barbosa, O.; Ortiz, C.; Binay, B.; Özdemir, E.; Gonçalves, L.R.B.; Fernandez-Lafuente, R. Easy stabilization of interfacially activated lipases using heterofunctional divinyl sulfone activated-octyl agarose beads. Modulation of the immobilized enzymes by altering their nanoenvironment. *Process Biochem.* **2016**, *51*, 865–874. [[CrossRef](#)]
7. Xu, L.; Ke, C.; Huang, Y.; Yan, Y. Immobilized *Aspergillus niger* lipase with SiO<sub>2</sub> nanoparticles in sol-gel materials. *Catalysts* **2016**, *6*, 149. [[CrossRef](#)]
8. Khoobi, M.; Motevalizadeh, S.F.; Asadgol, Z.; Forootanfar, H.; Shafiee, A.; Faramarzi, M.A. Synthesis of functionalized polyethylenimine-grafted mesoporous silica spheres and the effect of side arms on lipase immobilization and application. *Biochem. Eng. J.* **2014**, *88*, 131–141. [[CrossRef](#)]
9. Garcia-Galan, C.; Berenguer-Murcia, Á.; Fernandez-Lafuente, R.; Rodrigues, R.C. Potential of different enzyme immobilization strategies to improve enzyme performance. *Adv. Synth. Catal.* **2011**, *353*, 2885–2904. [[CrossRef](#)]
10. Mateo, C.; Palomo, J.M.; Fernandez-Lorente, G.; Guisan, J.M.; Fernandez-Lafuente, R. Improvement of enzyme activity, stability and selectivity via immobilization techniques. *Enzyme Microb. Technol.* **2007**, *40*, 1451–1463. [[CrossRef](#)]
11. Rodrigues, R.C.; Ortiz, C.; Berenguer-Murcia, A.; Torres, R.; Fernandez-Lafuente, R. Modifying enzyme activity and selectivity by immobilization. *Chem. Soc. Rev.* **2013**, *42*, 6290–6307. [[CrossRef](#)] [[PubMed](#)]
12. Fernandez-Lafuente, R. Stabilization of multimeric enzymes: Strategies to prevent subunit dissociation. *Enzyme Microb. Technol.* **2009**, *45*, 405–418. [[CrossRef](#)]
13. Barbosa, O.; Ortiz, C.; Berenguer-Murcia, A.; Torres, R.; Rodrigues, R.C.; Fernandez-Lafuente, R. Glutaraldehyde in bio-catalysts design: A useful crosslinker and a versatile tool in enzyme immobilization. *RSC Adv.* **2014**, *4*, 1583–1600. [[CrossRef](#)]
14. Badgujar, K.C.; Bhanage, B.M. Lipase immobilization on hydroxypropyl methyl cellulose support and its applications for chemo-selective synthesis of  $\beta$ -amino ester compounds. *Process Biochem.* **2016**, *51*, 1420–1433. [[CrossRef](#)]
15. Sikora, A.; Chelminiak-Dudkiewicz, D.; Siódmiak, T.; Tarczykowska, A.; Sroka, W.D.; Ziegler-Borowska, M.; Marszał, M.P. Enantioselective acetylation of (*R,S*)-atenolol: The use of *Candida rugosa* lipases immobilized onto magnetic chitosan nanoparticles in enzyme-catalyzed biotransformation. *J. Mol. Catal. B* **2016**, *134 Pt A*, 43–50. [[CrossRef](#)]

16. Karimi, M. Immobilization of lipase onto mesoporous magnetic nanoparticles for enzymatic synthesis of biodiesel. *Biocatal. Agric. Biotechnol.* **2016**, *8*, 182–188. [[CrossRef](#)]
17. Motevalzadeh, S.F.; Khoobi, M.; Sadighi, A.; Khalilvand-Sedagheh, M.; Pazhouhandeh, M.; Ramazani, A.; Faramarzi, M.A.; Shafiee, A. Lipase immobilization onto polyethylenimine coated magnetic nanoparticles assisted by divalent metal chelated ions. *J. Mol. Catal. B* **2015**, *120*, 75–83. [[CrossRef](#)]
18. Gupta, A.K.; Gupta, M. Synthesis and surface engineering of iron oxide nanoparticles for biomedical applications. *Biomaterials* **2005**, *26*, 3995–4021. [[CrossRef](#)] [[PubMed](#)]
19. Yang, Y.; Bai, Y.X.; Li, Y.F.; Lei, L.; Chui, Y.J.; Xia, C.G. Characterization of *Candida rugosa* lipase immobilized onto magnetic microspheres with hydrophilicity. *Process Biochem.* **2008**, *43*, 1179–1185. [[CrossRef](#)]
20. Ren, Y.; Rivera, J.G.; He, L.; Kulkarni, H.; Lee, D.-K.; Messersmith, P.B. Facile, high efficiency immobilization of lipase enzyme on magnetic iron oxide nanoparticles via a biomimetic coating. *BMC Biotechnol.* **2011**, *11*, 63. [[CrossRef](#)] [[PubMed](#)]
21. Marszałł, M.P.; Sroka, W.D.; Sikora, A.; Chelminiak, D.; Ziegler-Borowska, M.; Siódmiak, T.; Moaddel, R. Ligand fishing using new chitosan based functionalized Androgen receptor magnetic particles. *J. Pharm. Biomed. Anal.* **2016**, *127*, 129–135. [[CrossRef](#)] [[PubMed](#)]
22. Unsoy, G.; Yalcin, S.; Khodadust, R.; Gunduz, G.; Gunduz, U. Synthesis optimization and characterization of chitosan-coated iron oxide nanoparticles produced for biomedical applications. *J. Nanopart. Res.* **2012**, *14*, 964. [[CrossRef](#)]
23. Pan, Y.; Du, X.; Zhao, F.; Xu, B. Magnetic nanoparticles for the manipulation of proteins and cells. *Chem. Soc. Rev.* **2012**, *41*, 2912–2942. [[CrossRef](#)] [[PubMed](#)]
24. Skopinska-Wisniewska, J.; Olszewski, K.; Bajek, A.; Rynkiewicz, A.; Sionkowska, A. Dialysis as a method of obtaining neutral collagen gels. *Mater. Sci. Eng. C* **2014**, *40*, 65–70. [[CrossRef](#)] [[PubMed](#)]
25. Silva, J.A.; Macedo, G.P.; Rodrigues, D.S.; Giordano, R.L.C.; Gonçalves, L.R.B. Immobilization of *Candida antarctica* lipase B by covalent attachment on chitosan-based hydrogels using different support activation strategies. *Biochem. Eng. J.* **2012**, *60*, 16–24. [[CrossRef](#)]
26. Pandey, S.; Wilmer, E.N.; Morrell, D.S. Examining the efficacy and safety of squaric acid therapy for treatment of recalcitrant warts in children. *Pediatr. Dermatol.* **2015**, *32*, 85–90. [[CrossRef](#)] [[PubMed](#)]
27. Skopinska-Wisniewska, J.; Kuderko, J.; Bajek, A.; Maj, M.; Sionkowska, A.; Ziegler-Borowska, M. Collagen/elastin hydrogels cross-linked by squaric acid. *Mater. Sci. Eng. C* **2016**, *60*, 100–108. [[CrossRef](#)] [[PubMed](#)]
28. Sionkowska, A.; Kozłowska, J. Characterization of collagen/hydroxyapatite composite sponges as a potential bone substitute. *Int. J. Biol. Macromol.* **2010**, *47*, 483–487. [[CrossRef](#)] [[PubMed](#)]
29. Liu, L.; Xu, X.; Guo, S.; Han, W. Synthesis and self-assembly of chitosan-based copolymer with a pair of hydrophobic/hydrophilic grafts of polycaprolactone and poly(ethylene glycol). *Carbohydr. Polym.* **2009**, *75*, 401–407. [[CrossRef](#)]
30. Marszałł, M.P.; Siódmiak, T. Immobilization of *Candida rugosa* lipase onto magnetic beads for kinetic resolution of (R,S)-ibuprofen. *Catal. Commun.* **2012**, *24*, 80–84. [[CrossRef](#)]
31. Bradford, M.M. A rapid and sensitive method for the quantitation of microgram quantities of protein utilizing the principle of protein-dye binding. *Anal. Biochem.* **1976**, *72*, 248–254. [[CrossRef](#)]
32. Bakare, R.A.; Bhan, C.; Raghavan, D. Synthesis and characterization of collagen grafted poly(hydroxybutyrate-valerate) (PHBV) scaffold for loading of bovine serum albumin capped silver (AG/BSA) nanoparticles in the potential use of tissue engineering application. *Biomacromolecules* **2014**, *15*, 423–435. [[CrossRef](#)] [[PubMed](#)]
33. Jaiswal, N.; Prakash, O.; Talat, M.; Hasan, S.H.; Pandey, R.K.  $\alpha$ -Amylase immobilization on gelatin: Optimization of process variables. *J. Genet. Eng. Biotechnol.* **2012**, *10*, 161–167. [[CrossRef](#)]
34. Moreno-Perez, S.; Ghattas, N.; Filice, M.; Guisan, J.M.; Fernandez-Lorente, G. Dramatic hyperactivation of lipase of *Thermomyces lanuginosa* by a cationic surfactant: Fixation of the hyperactivated form by adsorption on sulfopropyl-sepharose. *J. Mol. Catal. B* **2015**, *122*, 199–203. [[CrossRef](#)]
35. Ghattas, N.; Filice, M.; Abidi, F.; Guisan, J.M.; Ben Salah, A. Purification and improvement of the functional properties of *Rhizopus oryzae* lipase using immobilization techniques. *J. Mol. Catal. B* **2014**, *110*, 111–116. [[CrossRef](#)]
36. Shang, C.-Y.; Li, W.-X.; Zhang, R.-F. Immobilization of *Candida rugosa* lipase on ZnO nanowires/macroporous silica composites for biocatalytic synthesis of phytosterol esters. *Mater. Res. Bull.* **2015**, *68*, 336–342. [[CrossRef](#)]

37. Hou, C.; Qi, Z.; Zhu, H. Preparation of core-shell magnetic polydopamine/alginate biocomposite for *Candida rugosa* lipase immobilization. *Colloids Surf. B* **2015**, *128*, 544–551. [[CrossRef](#)] [[PubMed](#)]
38. Mahto, T.K.; Chowdhuri, A.R.; Sahoo, B.; Sahu, S.K. Polyaniline-functionalized magnetic mesoporous nanocomposite: A smart material for the immobilization of lipase. *Polym. Compos.* **2016**, *37*, 1152–1160. [[CrossRef](#)]
39. Wang, J.; Zhao, G.; Jing, L.; Peng, X.; Li, Y. Facile self-assembly of magnetite nanoparticles on three-dimensional graphene oxide–chitosan composite for lipase immobilization. *Biochem. Eng. J.* **2015**, *98*, 75–83. [[CrossRef](#)]



© 2017 by the authors; licensee MDPI, Basel, Switzerland. This article is an open access article distributed under the terms and conditions of the Creative Commons Attribution (CC-BY) license (<http://creativecommons.org/licenses/by/4.0/>).